Effect of the VR-guided grasping task on the brain functional network

GUANGJIAN SHAO,[1,2] GONGCHENG XU,[2] (iD) CONGCONG HUO,[2] ZICHAO NIE,[2] YIZHENG ZHANG,[1] LI YI,[1] DONGYANG WANG,[1] ZHIYONG SHAO,[1] SHANFAN WENG,[3,4] JINYAN SUN,[3,5] (iD) AND ZENGYONG LI[2,6]

[1] *School of Mechatronic Engineering and Automation, Foshan University, Foshan, China*
[2] *Beijing Key Laboratory of Rehabilitation Technical Aids for Old-Age Disability, National Research Center for Rehabilitation Technical Aids, Beijing, China*
[3] *School of Medicine, Foshan University, Foshan, China*
[4] *13929998239@139.com*
[5] *jinyansun@fosu.edu.cn*
[6] *lizengyong@mca.gov.cn*

Abstract: Virtual reality (VR) technology has been demonstrated to be effective in rehabilitation training with the assistance of VR games, but its impact on brain functional networks remains unclear. In this study, we used functional near-infrared spectroscopy imaging to examine the brain hemodynamic signals from 18 healthy participants during rest and grasping tasks with and without VR game intervention. We calculated and compared the graph theory-based topological properties of the brain networks using phase locking values (PLV). The results revealed significant differences in the brain network properties when VR games were introduced compared to the resting state. Specifically, for the VR-guided grasping task, the modularity of the brain network was significantly higher than the resting state, and the average clustering coefficient of the motor cortex was significantly lower compared to that of the resting state and the simple grasping task. Correlation analyses showed that a higher clustering coefficient, local efficiency, and modularity were associated with better game performance during VR game participation. This study demonstrates that a VR game task intervention can better modulate the brain functional network compared to simple grasping movements and may be more beneficial for the recovery of grasping abilities in post-stroke patients with hand paralysis.

1. Introduction

Virtual Reality (VR) is a computer simulation system that creates a virtual world for simulated experiences [1]. VR technology involves interactive simulated environments that enhance users' engagement through appropriate sensory feedback and provide a realistic experience similar to the real world [2]. This immersive experience can motivate users to engage for longer periods and reduce the likelihood of boredom. In the context of VR games, users can engage in sensory-motor interactions. VR gaming platforms have been applied to motor function rehabilitation [3,4]. For better rehabilitation, the design of VR game paradigms needs to adhere to rehabilitation theories. Neural plasticity provides a theoretical basis for motor function rehabilitation in stroke patients [5]. Specifically, Cortical reorganization plays a crucial role in neural plasticity, and the significant reduction in limb activity following a stroke can lead to a decrease in neural plasticity [6].

Traditional limb rehabilitation treatments, such as hand-grasping function rehabilitation in post-stroke hemiparetic patients, often require the constant guidance and assistance of a rehabilitation therapist, which can be time-consuming and labor-intensive. Additionally, long periods of repetitive training without timely feedback may decrease patients' motivation and treatment

efficacy [4]. To address this issue, some studies have proposed incorporating virtual reality (VR) games into rehabilitation training to increase their enjoyment [7]. Moreover, the visual, tactile, and cognitive stimulation or feedback provided by virtual scenes and games can further enhance neural plasticity, influence brain network reorganization, and promote post-stroke motor function recovery [8]. Studies have demonstrated the effectiveness of VR game interventions in upper limb rehabilitation through assessments using tracking scales [9–12]. In addition, Silvia et al. [13] used electroencephalography (EEG) and compared the activation patterns in healthy subjects under different VR scenes. They discovered the VR game training scene mode that most effectively stimulates the motor cortex. Chen et al. [14] used EEG and electromyography techniques to record the relevant cortical potentials in the brain and muscle activity in the upper limbs of patients undergoing VR rehabilitation training and traditional therapy. They found that VR intervention was superior to the traditional therapy in improving cognitive neural processes related to movement expectation and reducing excessive compensatory activation in the contralateral cerebral hemisphere. Although the effectiveness of VR game intervention in improving limb function recovery has been demonstrated, the mechanisms underlying its impact on the cortical functional network of the brain are not yet clear.

The brain is a complex organ with interconnected regions that exhibit dynamic functional patterns [15]. Analyzing brain functional networks allows researchers to capture this complexity by considering the interactions and relationships between different brain regions, providing a comprehensive understanding of brain function [16,17]. By studying the organization and connectivity patterns of brain functional networks, researchers can develop models that may help predict individual cognitive performance or behavioral traits, contributing to personalized medicine and neuroscience. On the other hand, brain network information is associated with after-stroke motor function [18,19], and exploring the effect of VR on brain network function is conducive to understanding the mechanism of VR games in stroke rehabilitation.

Thus, this study aims to design a task-oriented hand function rehabilitation approach utilizing virtual game scenes and use fNIRS to investigate the influence of the VR-guided rehabilitation program on the brain functional network. fNIRS reflects brain function activity by measuring concentration changes of oxygenated and deoxygenated hemoglobin ($\Delta[HbO2]$ and $\Delta[Hb]$). fNIRS has the advantages of non-invasiveness, low cost, portability, minimal subject restriction, strong anti-interference capability, and low environmental requirements. It has become an important research tool in stroke rehabilitation [20–23]. We calculated the brain network topological properties based on the graph theory method, compared the differences in brain network regulation between VR rehabilitation training and traditional rehabilitation training and tried to establish a mapping relationship between VR rehabilitation training and motor performance behavior. This study can provide a theoretical basis for the further development of task paradigms suitable for rehabilitation training.

2. Materials and methods

2.1. Subjects

A total of 18 young healthy subjects were recruited (8 females and 10 males) to participate in this study. All subjects had no history of hypertension, severe illnesses, or traumatic brain injuries, and were able to actively perform grasping movements. Subjects with any of the following conditions were excluded: congenital deformities in any part of the body, infectious diseases, critical illnesses, or poor compliance. We collected information on the subjects' age, body mass index (BMI), and hand conditions (see Table 1). The experimental procedures were approved by the Ethics Committee of the National Rehabilitation Technology Assistance Research Center and were conducted in accordance with the ethical standards outlined in the 1975 Helsinki Declaration and its revised version in 2008. The clinical trial was registered under the number "ChiCTR210005148". All subjects provided informed consent before the formal experiment.

Table 1. Basic information of subjects

Parameters	Means (SD)
Age (years)	25.2 (1.9)
Body mass index (BMI)	21.21 (2.6)
Number of right-handed subjects	18 (0)

2.2. VR rehabilitation game

Repetitive grasping training is beneficial for hand function recovery [24]. Repetitive rehabilitation training helps patients establish new connections between their limbs and the central nervous system, leading to effective rehabilitation outcomes [25]. And the high-interest task paradigms can induce strong movement-performing intentions [26]. Based on virtual scenes, we have developed a specific task-oriented rehabilitation training paradigm for stroke patients [27], aiming to improve patients' initiative and enthusiasm in rehabilitation training and promote their hand function recovery.

The VR rehabilitation game scenes were designed using Unity3D. In the game, subjects were induced to perform continuous grasping movements by following a repetitive motion track. Subjects controlled a ball in the game to avoid obstacles by extending and flexing their fingers and obtained scoring points in this process. To minimize testing variables, the arrangement of tracks was a repetitive trajectory. The game scenes are shown in Fig. 1(a). We used a data glove (Fig. 1(a)) to capture the joint angle movements of the subjects' hands, which were then used to control the left and right movement of the ball in the game. Additionally, we recorded the game duration, finger bending angles, the real-time coordinates of the ball, and the coordinates of the
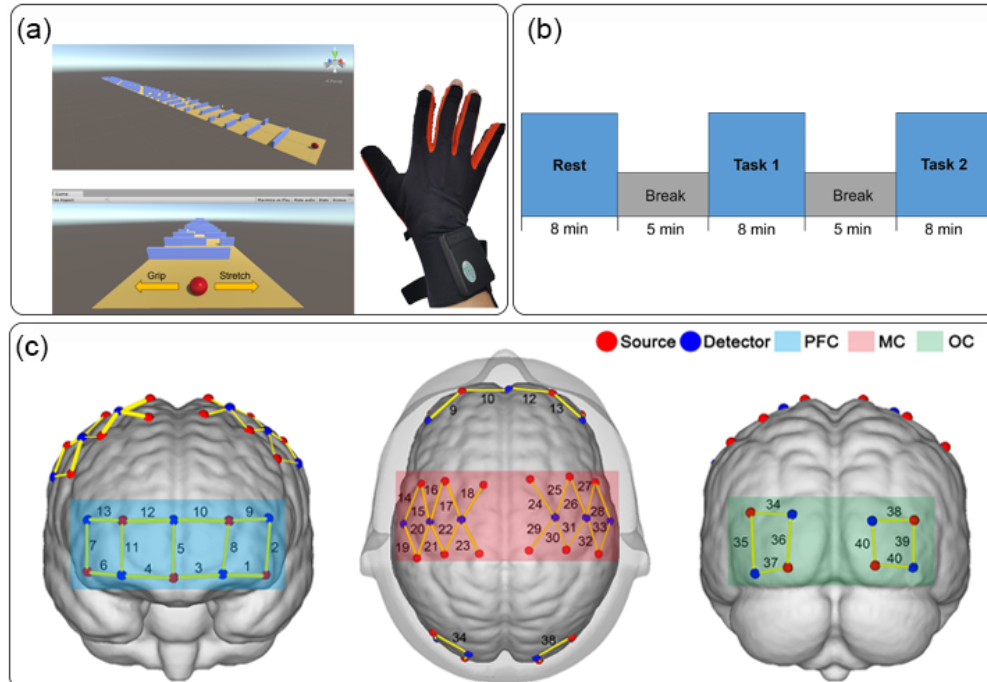

Fig. 1. Experimental setup. (a) Game scenes and VR data gloves. (b) Experimental procedure. (c) fNIRS-measured brain area schematic diagram. The blue area represents PFC, the red area represents MC, and the green area represents OC.

channel track. The accuracy of subjects completing the game can be determined by calculating the difference between the real-time coordinates of the ball and the coordinates of the midpoint of the channel track.

2.3. Experimental procedures

In the experiment, participants were scheduled to undergo rest and two task conditions: (Task 1) a simple grasping task and (Task 2) a VR game-directed grasping task. Before the experiment, participants had at least 10 minutes of practice to familiarize themselves with the game operation in Task 2. They were required to successfully guide the ball through 95% of the channels in a single grasping motion [28], ensuring they had learned the game operation. The experiment was conducted in a quiet room. During the rest condition, participants closed their eyes, remained awake and maintained a relaxed sitting position for eight minutes. After a 5-minute break, they performed eight minutes of continuous grasping training without the game guidance. After another 5-minute break, they performed eight minutes of continuous grasping training with the game guidance. In Task 2, participants controlled the ball in the game by performing continuous grasping motions, following a pre-set track in the form of a periodic trajectory. Participants were required to complete one grasping motion each period. The experimental procedure is illustrated in Fig. 1(b). To minimize testing variables, no sound was added to the game.

2.4. fNIRS data collection

We used the multi-channel fNIRS imaging device (NirSmart, Danyang Huicuang Medical Equipment Co., Ltd., China) to collect brain hemodynamic signals during the experiment. A continuous-wave fNIRS system using wavelengths of 760 and 850 nm was utilized to collect the fNIRS data at a sampling rate of 10 Hz. The differential path-length factors (DPFs) were set to 6. The emitter-detector distance was 3 cm. We determined the specific brain regions of interest based on the cortical areas involved in grasping movements and game task execution. The prefrontal cortex (PFC) is commonly considered the center of human cognitive functions, involved in information processing such as working memory and attention allocation [18,29]. The motor cortex (MC) is responsible for perceiving body posture and movement and controlling movements of the contralateral limbs and plays a significant role in sensation and motor control [30–32]. The occipital cortex (OC) is primarily involved in visual information processing and is also associated with functions such as memory and motion perception [33]. In our task-oriented grasping game, visual observation is required to obtain the movement trajectory, followed by decision-making and execution based on the observed trajectory. This involves visual information processing, cognition, attention allocation, and limb movement execution. Therefore, we selected six brain regions of interest, including the left and right prefrontal cortex (LPFC, RPFC), left and right motor cortex (LMC, RMC), and left and right occipital cortex (LOC, ROC). These six brain regions and their channel distribution, arranged according to the 10/10 international system [34], are shown in Fig. 1(c).

2.5. fNIRS data processing

2.5.1. fNIRS data preprocessing

We preprocessed the data using the MATLAB software. Firstly, we applied the modified Lambert-Beer law to obtain $\Delta[HbO2]$ and extracted the hemodynamic parameters for each task condition [35]. The $\Delta[HbO2]$ variable appeared to be sufficiently sensitive for representation of information processing in the cortical region, whereas the combination of these two variables only improves slight performance in some cases [36]. Therefore, only $\Delta[HbO2]$ signal was used for analyses in this study. Then, we employed the Time Derivative Distribution Repair (TDDR) algorithm [37,38] to remove the baseline drifts and peak artifacts. Since superficial artifacts affect every channel as a global interference signal, we applied the Common Average Reference

(CAR) spatial filtering method [39,40], and calculated the mean value across all channels and subtracted this value from each channel at each time point to reduce the impact of the superficial artifacts [39,41]. Finally, we applied a bandpass filter to obtain the fNIRS signals in the range of 0.01-0.1 Hz [42].

2.5.2. Graph theory-based brain network properties

In this study, we used fNIRS channels as nodes and the functional connections between channels as edges, and constructed an undirected and unweighted graph theoretical network analysis. The instantaneous phase for each fNIRS channel was obtained by using the Hilbert transform, and the Phase-locking value (PLV) [43,44] between every pair of channels was used to construct the correlation matrix, denoted as

$$m_{plv} = \begin{bmatrix} PLV_{1\,1} & \cdots & PLV_{1\,ch} \\ \vdots & \ddots & \vdots \\ PLV_{ch\,1} & \cdots & PLV_{ch\,ch} \end{bmatrix}, \tag{1}$$

where ch represents the number of channels. The PLV between channel a and channel b is defined as

$$PLV_{a\,b} = \left| \frac{1}{N} \sum_{n=1}^{N} \exp(j(\varphi_a[n] - \varphi_b[n])) \right|, \tag{2}$$

where $\varphi[n]$ is the instantaneous phase for the nth sampling point of a certain channel, and N is the number of sampling points for that channel. In this manner, we obtained the PLV-based functional connectivity network of samples

Next, we obtained the corresponding binary network from the correlation matrix by applying different sparsity thresholds. We chose a threshold range of 0.2-0.6 with a step size of 0.02. The elements in the upper or lower triangle of the m_{plv} matrix were sorted in descending order, and elements greater than the threshold were set to 1, while the rest were set to 0. For example, at a threshold of 0.4, the top 60% of correlations were defined as 1, indicating a connection between those two channels in graph theory. Finally, using the Brain Connectivity Toolbox (BCT), graph theoretical measures were computed, including clustering coefficient (C), characteristic path length (Lp), global efficiency (GE), local efficiency (LE), transitivity (T), and small-worldness (δ) [45].

(1) The clustering coefficient (C_i) of a node represents the degree of connectivity between the node and its neighbors. The network's C is the average of all the node clustering coefficients, and it reflects the local clustering and isolation degree of the entire network. It is given as

$$C = \frac{1}{m} \sum_{i=1}^{m} C_i = \frac{1}{m} \sum_{i=1}^{m} \frac{2e_i}{K_i(K_i - 1)}, \tag{3}$$

where C_i represents the clustering coefficient of node i, e_i represents the number of directly connected neighboring nodes to node i, K_i represents the degree of node i, and m is the total number of nodes.

(2) Lp is defined as the minimum number of edges required to connect any two nodes in the network. It represents the average path length of all nodes in the network, given by

$$Lp = \frac{1}{m(m - 1)} \sum_{x,y \in m, x \neq y} d_{x,y}, \tag{4}$$

where the shortest path length $d_{x,y}$ refers to the minimum number of edges required to connect nodes x and y.

(3) GE: A shorter path length implies lower energy consumption and higher efficiency in information transfer. The global effect is the mean value of the reciprocal of the shortest path length ($d_{x,y}$) of all nodes.

$$GE = \frac{1}{m(m-1)} \sum_{x,y \in m, x \neq y} \frac{1}{d_{x,y}}, \qquad (5)$$

(4) LE: While global efficiency is a metric for assessing the overall efficiency of information transmission in the network, it is possible to have nodes that are not directly connected. Local efficiency is used to provide a more comprehensive evaluation of network efficiency. It is the mean efficiency of the subgraph G_i, which consists of all of the neighboring nodes for each node and is calculated as

$$LE = \frac{1}{m} \sum_{i=1}^{m} E(G_i), \qquad (6)$$

(5) T: It refers to the ratio of the number of triangles (closed triples) to the number of triples (three nodes that have connections) in the network. It is given as

$$T = \frac{Triangle\ number}{Triple\ number}, \qquad (7)$$

(6) M: In brain networks, modularity refers to the extent of functional specialization and mutual influence between different regions of the brain. A high level of modularity implies that different brain regions operate more independently and have less impact on each other when performing specific tasks. In this study, we evaluated the modularity of the brain network using the Louvain algorithm [46].

(7) To calculate the small-worldness measure δ, we first need to compute the normalized clustering coefficient γ and the normalized characteristic path length λ. The ratio of γ to λ gives us the small-worldness measure δ:

$$\gamma = \frac{C}{C_r}, \qquad (8)$$

$$\lambda = \frac{L}{L_r}, \qquad (9)$$

$$\delta = \frac{\gamma}{\lambda}, \qquad (10)$$

Here, C_r and L_r represent the average clustering coefficient and characteristic path length of 200 randomly generated networks, respectively.

(8) The average clustering coefficient and average local efficiency of each brain region were calculated by averaging the clustering coefficients and local efficiencies of each channel in the six br.in regions: LPFC, RPFC, LMC, RMC, LOC, and ROC. They are respectively defined as C_{LPFC}., C_{RPFC}, C_{LMC}, C_{RMC}, C_{LOC}, C_{ROC}, LE_{LPFC}, LE_{RPFC}., LE_{LOC}., LE_{ROC}, LE_{LMC}, LE_{ROC}.

2.6. Hand function performance under the VR-game task

During the gaming task, we recordedarticipants' rl-time game performance at the sampling rate of 10 Hz, including the x-coordinate of the standard path (standard path $d_s[n]$) and the real-time x-coordinate of the movement of the game character under the participants' control (actual movement trajectory $d_r[n]$). We then calculated the following metrics as evaluation indicators for the participants' hand rehabilitation training under the game guidance:

(1) The mean (*DDM*) and standard deviation (*DDS*) of the difference between the standard path and the actual movement trajectory:

$$DDM = \frac{1}{n}\left|\sum_{i=1}^{n}\Delta d_i\right|,\tag{11}$$

$$DDS = \sqrt{\frac{1}{n}\sum_{i=1}^{n}(\Delta d_i - \Delta d_m)^2},\tag{12}$$

where Δd_i represents the difference between the x-coordinate of the standard path and the x-coordinate of the actual movement trajectory at the i-th data point, mathematically represented as $\Delta d_i = d_s[i] - d_r[i]$. Δd_m is the mean of $|\Delta d_i|$, $\Delta d_m = \frac{1}{n}\sum_{i=1}^{n}|\Delta d_i|$.

(2) The mean (*VDM*) and standard deviation (*VDS*) of the velocity difference between the standard path and the actual movement trajectory:

$$VDM = \frac{1}{n}\left|\sum_{i=1}^{n-1}\Delta v_i\right|,\tag{13}$$

$$VDS = \sqrt{\frac{1}{n}\sum_{i=1}^{n-1}(\Delta v_i - \Delta v_m)^2},\tag{14}$$

where Δv_i represents the velocity difference: $\Delta v_i = v_s[i] - v_r[i]$. Δv_m is the mean of $|\Delta v_i|$: $\Delta v_m = \frac{1}{n}\sum_{i=1}^{n}|\Delta v_i|$.

(3) The mean (*ADM*) and standard deviation (*ADS*) of the acceleration difference between the standard path and the actual movement trajectory:

$$ADM = \frac{1}{n}\left|\sum_{i=1}^{n-1}\Delta a_i\right|,\tag{15}$$

$$ADS = \sqrt{\frac{1}{n}\sum_{i=1}^{n-1}(\Delta a_i - \Delta a_m)^2},\tag{16}$$

where Δa_i represents the ratio between the velocity difference Δa_m is the mean of $|\Delta a_i|$: $\Delta a_m = \frac{1}{n}\sum_{i=1}^{n}|\Delta a_i|$.

These above parameters related to game performance were used to characterize the participants' accuracy in controlling the game character. They reflected the relationship between hand movements during the game and the guidance provided by the game. Smaller values of these parameters indicated a closer alignment between hand movements and the game guidance, reflecting participants' better motor control ability.

2.7. Statistical analyses

One-way analysis of variance (ANOVA) was used to compare the network properties (C, Lp, GE, LE, M, T) among the three tasks at each threshold. Then, multiple comparisons were conducted to confirm differences in network properties between each two tasks. Pearson correlation analyses were performed to explore the relationship between game performance parameters and the average clustering coefficients and local efficiencies of each brain region and the whole brain network properties. The Pearson correlation and ANOVA analyses were conducted using the MATLAB software. The level of statistical significance was set at 0.05.

3. Results

3.1. Task-related changes in the whole topological metrics

The six network properties obtained from all measured brain regions for the three tasks are shown in Fig. 2. All these six network properties change with the threshold increase. At lower thresholds, more channels were connected. As the threshold increased, the number of connections decreased. This led to a decrease in C and an increase in Lp. GE, LE and T decreased with increasing thresholds. With higher thresholds, weaker PLV connections were disconnected, reducing the number of closed triplets in the network and increasing the degree of M. If a network exhibits small-world characteristics, the small-worldness δ should be greater than one [45]. It can be seen from Fig. 3 that the brain networks in the three tasks demonstrated small-world features.
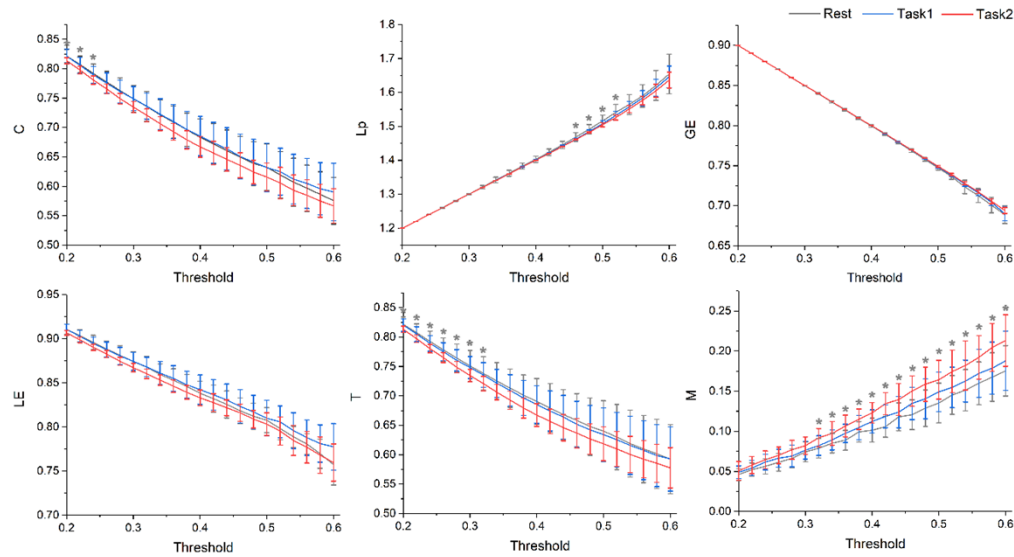

Fig. 2. The six network properties for the three tasks under each threshold. The asterisk (*) indicates a significant difference (p < 0.05) between VR game-guided grasping movement and the resting state.
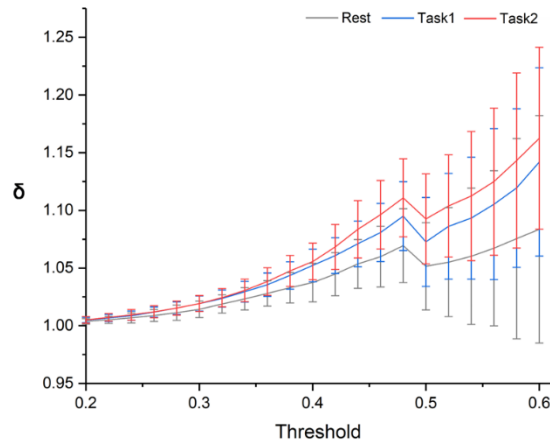

Fig. 3. The small-worldness of the brain networks in the three tasks

One-way ANOVA revealed that the task effect was significant on C, Lp, LE, T, M, and δ at certain thresholds. Further multiple comparisons showed that, compared to the resting state, Task 2 exhibited higher M and δ, and lower C, Lp, LE, and T at certain thresholds, as shown in Fig. 2. There were no significant differences between Task 2 and Task 1 on the seven network properties.
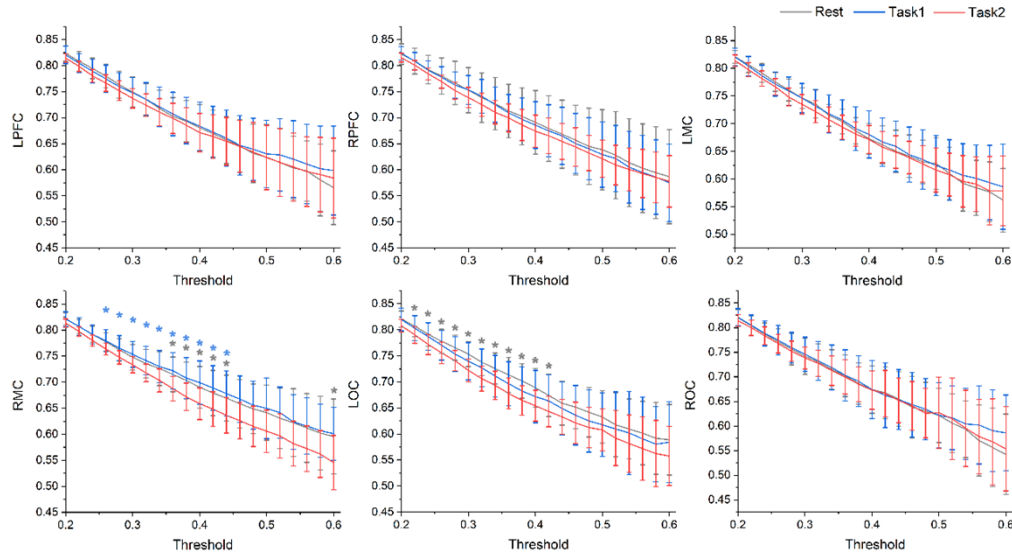

Fig. 4. The average clustering coefficients for each brain region under the three tasks. The gray asterisk (*) indicates significant differences (p < 0.05) between VR game-guided grasp motion and resting state. The blue asterisk (*) denotes significant differences (p < 0.05) between VR game-guided grasp motion and simple grasping motion.

Fig. 5. The average local efficiencies for each brain region under the three tasks. The gray asterisk (*) indicates significant differences (p < 0.05) between VR game-guided grasp motion and resting state. The blue asterisk (*) denotes significant differences (p < 0.05) between VR game-guided grasp motion and simple grasping motion.
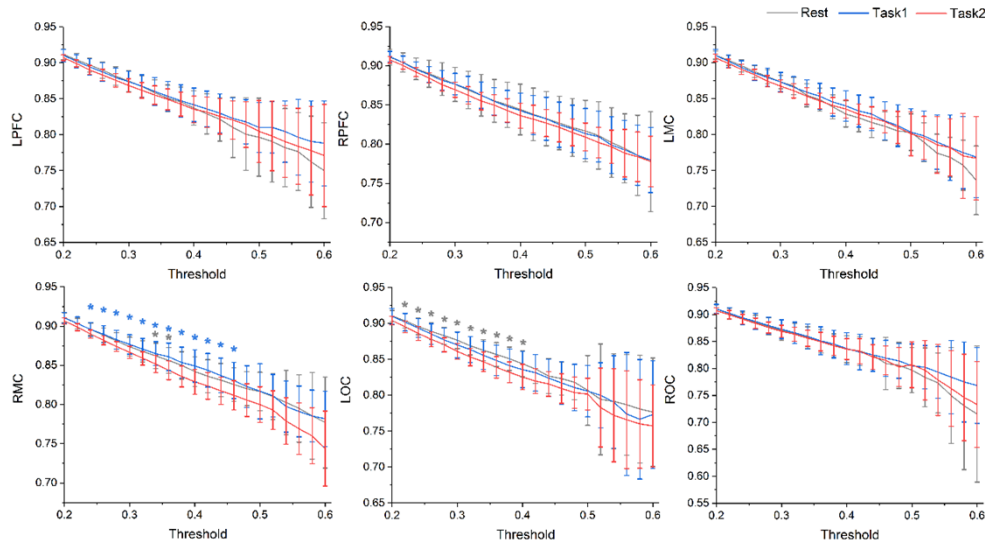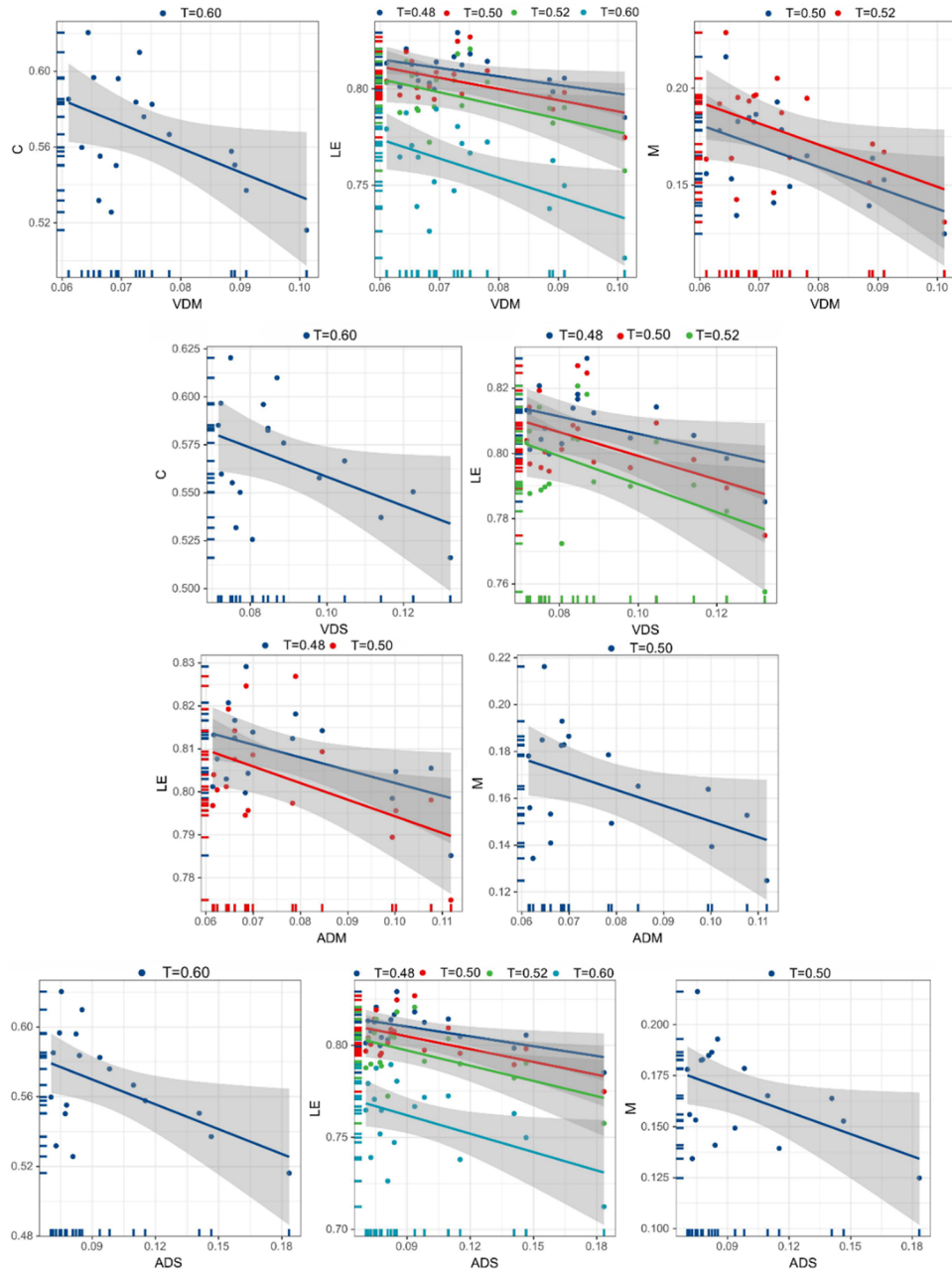
Fig. 6. The Scatter plot of the significant correlation between the whole brain network properties and peripheral limb performances. T represents the threshold.

Table 2. Correlation between peripheral limb performances and the whole brain network properties. T represents the threshold.

Peripheral limb performances	Brain network properties	T	r^2	p
VDM	C	0.6	0.235	0.041
	LEs	0.48	0.245	0.037
		0.5	0.254	0.032
		0.52	0.231	0.043
		0.6	0.277	0.025
	M	0.5	0.259	0.030
		0.52	0.299	0.044
VDS	C	0.6	0.235	0.048
	LE	0.48	0.230	0.040
		0.5	0.267	0.028
		0.52	0.243	0.038
ADM	LE	0.48	0.248	0.036
		0.5	0.256	0.032
	M	0.5	0.223	0.048
ADS	C	0.6	0.248	0.036
	LE	0.48	0.311	0.016
		0.5	0.321	0.014
		0.52	0.298	0.019
		0.6	0.245	0.037
	M	0.5	0.228	0.045

3.2. Task-related changes in the network metrics of each brain region

To further explore the involvement of each brain region in the tasks, we also compared the clustering coefficient and local efficiency for each brain region among the three tasks. One-way ANOVA showed significant task effect on C_{RMC}, LE_{RMC}, C_{LOC}, LE_{LOC}. Further multiple comparisons revealed that Task 2 showed a decrease of C_{RMC}, LE_{RMC} compared to the resting state and Task 1 (Fig. 4 and 5). Additionally, Task 2 also had a lower C_{LOC}, LE_{LOC} compared to the resting state (Fig. 4 and 5).

3.3. Correlation results

To better understand the quantitative relationship between subjects' peripheral limb performances and changes in brain network properties, we conducted correlation analyses. Figure 6 presents all the significant correlations between the limb performance and the whole network properties ($p < 0.05$). Specifically, VDM was negatively correlated with C, LE and M. VDS was negatively correlated with C and LE. ADM was negatively correlated with the LE and M. ADS had a negative correlation with the C, LE and M. The values of r^2 and p for these significant correlations are shown in Table 2.

Besides, we analyzed the correlation between subjects' peripheral limb performances and the average clustering coefficient and local efficiency for each brain region. We found significant correlations primarily in the LPFC, followed by the RMC (Fig. 7 and 8). The values of r^2 and p for these significant correlations are presented in Table 3 and Table 4.
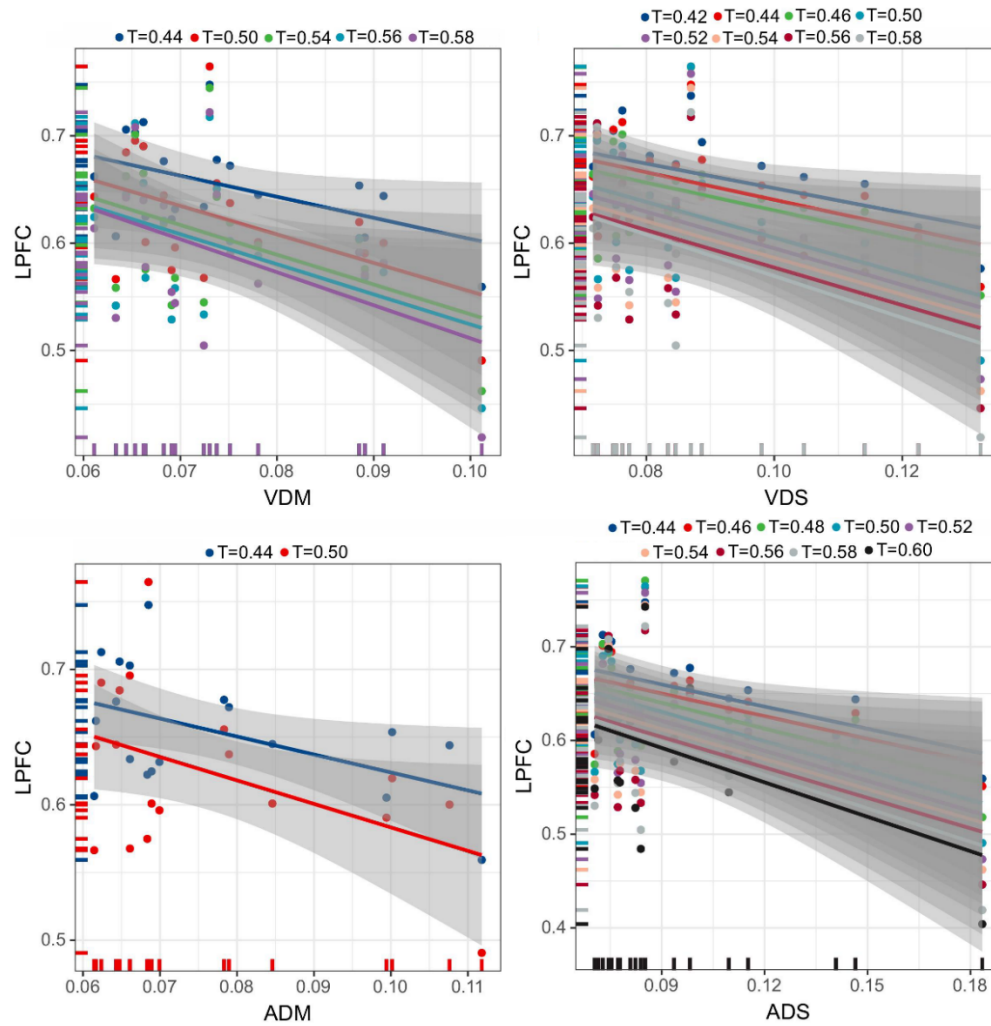
Fig. 7. The Scatter plot of the significant correlation between the average C of each brain region and peripheral limb performances. T represents the threshold.
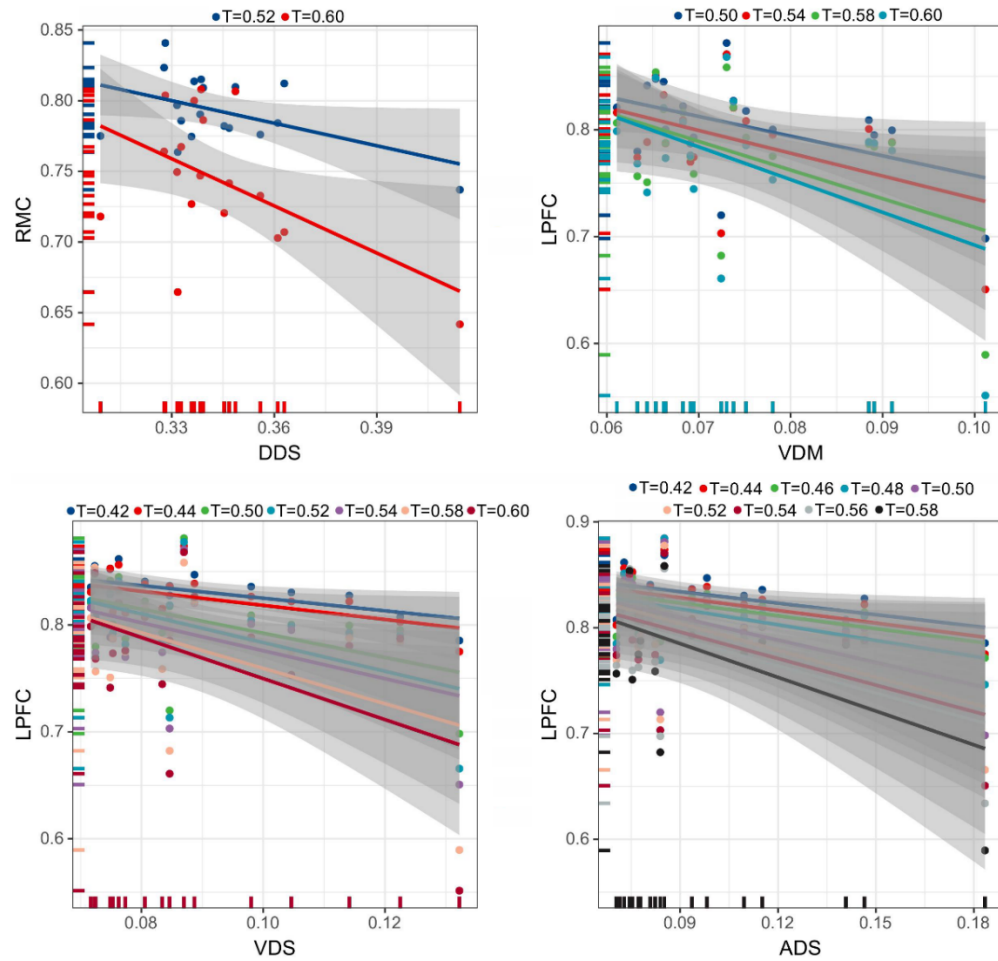
Fig. 8. The Scatter plot of the significant correlation between the average LE of each brain region and peripheral limb performances. T represents the threshold.

Table 3. Correlation between peripheral limb performances and average clustering coefficient and local efficiency of each brain region. T represents the threshold.

	C					LE			
Limb performances	Brain regions	T	r^2	p	Limb performances	Brain regions	T	r^2	p
VDM	LPFC	0.44	0.233	0.042	DDS	RMC	0.52	0.221	0.049
		0.5	0.230	0.044			0.6	0.258	0.031
		0.54	0.228	0.045	VDM	LPFC	0.5	0.228	0.045
		0.56	0.220	0.049			0.54	0.228	0.045
		0.58	0.232	0.044			0.58	0.236	0.041
VDS	LPFC	0.42	0.250	0.035			0.6	0.232	0.043
		0.44	0.264	0.029	VDS	LPFC	0.42	0.256	0.032
		0.46	0.224	0.048			0.44	0.237	0.040
		0.50	0.230	0.039			0.5	0.228	0.045
		0.52	0.227	0.046			0.52	0.252	0.034
		0.54	0.228	0.045			0.54	0.228	0.045
		0.56	0.227	0.046			0.58	0.239	0.040
		0.58	0.243	0.038			0.6	0.240	0.039
ADM	LPFC	0.44	0.237	0.041	ADS	LPFC	0.42	0.286	0.022
		0.5	0.220	0.049			0.44	0.258	0.031
ADS	LPFC	0.44	0.296	0.020			0.46	0.225	0.047
		0.46	0.257	0.032			0.48	0.239	0.038
		0.48	0.255	0.032			0.5	0.263	0.029
		0.5	0.279	0.024			0.52	0.299	0.019
		0.52	0.266	0.029			0.54	0.278	0.025
		0.54	0.267	0.028			0.56	0.259	0.031
		0.56	0.259	0.031			0.58	0.291	0.020
		0.58	0.270	0.027					
		0.6	0.252	0.034					

4.   Discussion

This study utilized fNIRS to investigate the effects of VR game rehabilitation training on brain networks and the potential links between brain networks and game performance. The results showed that the VR game induced higher modularity and lower C, Lp, and T than the resting state. Besides, the C_{RMC}, LE_{RMC} for the VR game task were significantly lower than those of Task 1. In game-based rehabilitation training, game performance was significantly negatively correlated with the brain network's C, LE, and M. It was also significantly negatively correlated with C_{LPFC}, LE_{LPFC} and LE_{RMC}.

4.1.   Decrease in clustering coefficient of the whole brain and each region

In this study, compared to the resting state, the clustering coefficient and transitivity of the brain network decreased during game task-oriented conditions, indicating a reduction in the number of local short connections in the brain network. Pang [18] and Lin [19] compared the functional brain networks of healthy subjects and post-stroke patients with motor impairments in the prefrontal cortex and motor areas, respectively. They found that the clustering coefficient and transitivity in the motor cortex of stroke patients were significantly higher than those in healthy participants, indicating a phenomenon of high local clustering in the brain functional network of stroke patients. The reduction in the number of local short connections observed during VR game task-oriented rehabilitation training suggests that the VR rehabilitation training designed in this study may be an effective approach for stroke rehabilitation. The clustering coefficients in the RMC and LOC brain regions were lower than in the resting state. Moreover, compared to simple grasping movements, VR intervention significantly decreased the average clustering coefficient in the RMC brain region. These results suggest that VR game-oriented grasping movements can reduce the average clustering coefficient of the entire brain and significantly decrease the clustering coefficient in the motor cortex after excluding the effects of grasping alone. This indicates that VR game intervention can improve the brain functional network to some extent and may help improve the efficiency of grip function rehabilitation in patients. Previous research has shown that with increasing task difficulty, due to the activation level of the brain and the reallocation of brain resources, the functional connections of the contralateral brain region controlling unilateral movements are inhibited [28,47]. In task-oriented game conditions, the inhibition of functional connections leads to a reduction in local network connections, resulting in a decrease in the clustering coefficient. This finding is consistent with our previous research [27].

4.2.   Increase in modularity of the whole brain

The modularity of the brain network is associated with cognitive load in working memory [48–50]. Research has shown that the connectivity between different modules of the brain functional network changes as the cognitive demands of a task shift from simple to complex [51], leading to a dynamic transition of the brain's functional pattern from the default mode to task-positive states [52]. We believe that the inclusion of VR games increases the cognitive load during grasping movements for the participants, which is reflected in an increased modularity of the brain functional network. This phenomenon may be associated with the participants' increased engagement and active involvement in the task. One possible reason for the increase in modularity in a brain network is the functional segregation and specialization of different brain regions, where modules emerge to perform specific cognitive functions. This modular organization allows for efficient information processing and promotes robustness and flexibility in the brain [53]. However, the global efficiency and the local efficiency of the whole brain are reduced in this study. It may be due to the increase in functional specialization [54]. With modules form and become more distinct, there can be a decrease in the interconnectivity among

different brain regions within each module. This reduction in local connectivity can lead to a decrease in local efficiency.

4.3. Negative correlation between the game performance and brain network performances

DDM, DDS, VDM, VDS, ADM, and ADS can represent the stability of hand movement control to some extent. Higher values of these metrics indicate poorer control stability. Higher values of the average clustering coefficient, average local efficiency, and modularity at the whole-brain level corresponded to lower game performance, indicating more accurate and stable game performance. This suggests that in VR game tasks, better performance depends on a greater number of connections within and between modules, which is consistent with the findings of [55]. Higher local efficiency and clustering coefficient may be associated with a stronger ability of the network to process information.

4.4. Limitations and future directions

During the experimental design phase, we did not randomize the order of the tasks. However, randomizing the experimental sequence would have been more advantageous for this study. To minimize testing variables, we did not introduce any additional sounds in each experiment. However, this led to a certain degree of mismatch between the grasping actions and VR grasping actions in terms of frequency. This will require improvements in future projects. The following study will focus on stroke patients. The CAR algorithm was used to reduce the superficial artifacts in this study. Short-distance measurements as regressors in a General Linear Model (GLM) has been proved to be more efficient in removing systemic interference [56,57], we will try to improve the reliability of the data by adopting short-distance channels in the future study.

5. Conclusion

In this study, our designed VR game task intervention can decrease the clustering coefficient of the brain motor cortex network and enhance the modularity of the whole brain network. This suggests that VR game task-oriented grasping training may potentially improve the pathological features characterized by a high clustering coefficient in the motor cortex while enhancing the patient's ability to mobilize brain resources for brain network remodeling.

Disclosures. The authors declare no conflicts of interest.

Data availability. Data underlying the results presented in this paper are not publicly available at this time but may be obtained from the authors upon reasonable request.

References

1. L. Wang, J. L. Chen, A. M. K. Wong, *et al.*, "Game-Based Virtual Reality System for Upper Limb Rehabilitation After Stroke in a Clinical Environment: Systematic Review and Meta-Analysis," Games Health J **11**(5), 277–297 (2022).
2. K. R. Lohse, C. G. Hilderman, K. L. Cheung, *et al.*, "Virtual reality therapy for adults post-stroke: a systematic review and meta-analysis exploring virtual environments and commercial games in therapy," PLoS One **9**(3), e93318 (2014).
3. S. Ikbali Afsar, I. Mirzayev, O. Umit Yemisci, *et al.*, "Virtual Reality in Upper Extremity Rehabilitation of Stroke Patients: A Randomized Controlled Trial," J Stroke Cerebrovasc Dis **27**(12), 3473–3478 (2018).
4. M. A. Ahmad, D. K. A. Singh, N. A. Mohd Nordin, *et al.*, "Virtual Reality Games as an Adjunct in Improving Upper Limb Function and General Health among Stroke Survivors," Int. J. Environ. Res. Public Health **16**(24), 5144 (2019).

5. M. A. Dimyan and L. G. Cohen, "Neuroplasticity in the context of motor rehabilitation after stroke," Nat. Rev. Neurol. **7**(2), 76–85 (2011).
6. B. B. Johansson, "Current trends in stroke rehabilitation. A review with focus on brain plasticity," Acta Neurol Scand **123**(3), 147–159 (2011).
7. M. G. Lansberg, C. Legault, A. MacLellan, *et al.*, "Home-based virtual reality therapy for hand recovery after stroke," PM R **14**(3), 320–328 (2022).
8. S. H. You, S. H. Jang, Y. H. Kim, *et al.*, "Virtual reality-induced cortical reorganization and associated locomotor recovery in chronic stroke: an experimenter-blind randomized study," Stroke **36**(6), 1166–1171 (2005).
9. P. Dominguez-Tellez, J. A. Moral-Munoz, A. Salazar, *et al.*, "Game-Based Virtual Reality Interventions to Improve Upper Limb Motor Function and Quality of Life After Stroke: Systematic Review and Meta-analysis," Games Health J **9**(1), 1–10 (2020).
10. M. Maier, B. Rubio Ballester, A. Duff, *et al.*, "Effect of Specific Over Nonspecific VR-Based Rehabilitation on Poststroke Motor Recovery: A Systematic Meta-analysis," Neurorehabil Neural Repair **33**(2), 112–129 (2019).
11. K. Adie, C. Schofield, M. Berrow, *et al.*, "Does the use of Nintendo Wii Sports(TM) improve arm function? Trial of Wii(TM) in Stroke: a randomized controlled trial and economics analysis," Clin Rehabil **31**(2), 173–185 (2017).
12. K. E. Laver, B. Lange, S. George, *et al.*, "Virtual reality for stroke rehabilitation," Cochrane Database Syst Rev **2018**(1), CD008349 (2017).
13. S. E. Kober, V. Settgast, M. Brunnhofer, *et al.*, "Move your virtual body: differences and similarities in brain activation patterns during hand movements in real world and virtual reality," Virtual Reality **26**(2), 501–511 (2022).
14. L. Chen, Y. Chen, W. B. Fu, *et al.*, "The Effect of Virtual Reality on Motor Anticipation and Hand Function in Patients with Subacute Stroke: A Randomized Trial on Movement-Related Potential," Neural Plast **2022**, 1–14 (2022).
15. A. R. Carter, G. L. Shulman, and M. Corbetta, "Why use a connectivity-based approach to study stroke and recovery of function?" NeuroImage **62**(4), 2271–2280 (2012).
16. A. G. Guggisberg, P. J. Koch, F. C. Hummel, *et al.*, "Brain networks and their relevance for stroke rehabilitation," Clin. Neurophysiol. **130**(7), 1098–1124 (2019).
17. J. S. Siegel, B. A. Seitzman, L. E. Ramsey, *et al.*, "Re-emergence of modular brain networks in stroke recovery," Cortex **101**, 44–59 (2018).
18. R. Pang, D. Wang, T. S. R. Chen, *et al.*, "Reorganization of prefrontal network in stroke patients with dyskinesias: evidence from resting-state functional near-infrared spectroscopy," J Biophotonics **15**(7), e202200014 (2022).
19. S. Lin, D. Wang, H. Sang, *et al.*, "Predicting poststroke dyskinesia with resting-state functional connectivity in the motor network," Neurophotonics **10**(02), 025001 (2023).
20. P. M. Arenth, J. H. Ricker, and M. T. Schultheis, "Applications of functional near-infrared spectroscopy (fNIRS) to Neurorehabilitation of cognitive disabilities," Clin Neuropsychol **21**(1), 38–57 (2007).
21. A. Wong, L. Robinson, S. Soroush, *et al.*, "Assessment of cerebral oxygenation response to hemodialysis using near-infrared spectroscopy (NIRS): Challenges and solutions," J. Innov. Opt. Health Sci. **14**(06), 2150016 (2021).
22. M. Mihara and I. Miyai, "Review of functional near-infrared spectroscopy in neurorehabilitation," Neurophotonics **3**(3), 031414 (2016).
23. J. Sun, R. Pang, S. Chen, *et al.*, "Near-infrared spectroscopy as a promising tool in stroke: Current applications and future perspectives," J. Innovative Opt. Health Sci. **14**(06), 2130006 (2021).
24. S. Park, M. Fraser, L. M. Weber, *et al.*, "User-Driven Functional Movement Training With a Wearable Hand Robot After Stroke," IEEE Trans. Neural Syst. Rehabil. Eng. **28**(10), 2265–2275 (2020).
25. A. Basteris and S. Nijenhuis, "Training modalities in robot-mediated upper limb rehabilitation in stroke: a framework for classification based on a systematic review," J NeuroEngineering Rehabil **11**(1), 111 (2014).
26. C. Pengcheng and G. Nuo, "Research of VR-BCI and Its Application in Hand Soft Rehabilitation Ssystem," presented at *the 2021 IEEE 7th International Conference on Virtual Reality (ICVR)* 2021.
27. X. Li, J. Yin, H. Li, *et al.*, "Effects of Ordered Grasping Movement on Brain Function in the Performance Virtual Reality Task: A Near-Infrared Spectroscopy Study," Front. Hum. Neurosci. **16**, 798416 (2022).
28. C. M. Buetefisch, K. P. Revill, L. Shuster, *et al.*, "Motor demand-dependent activation of ipsilateral motor cortex," J Neurophysiol **112**(4), 999–1009 (2014).
29. K. Mandrick, G. Derosiere, G. Dray, *et al.*, "Prefrontal cortex activity during motor tasks with additional mental load requiring attentional demand: a near-infrared spectroscopy study," Neurosci. Res. **76**(3), 156–162 (2013).
30. A. K. Rehme, S. B. Eickhoff, C. Rottschy, *et al.*, "Activation likelihood estimation meta-analysis of motor-related neural activity after stroke," NeuroImage **59**(3), 2771–2782 (2012).
31. Y. Zhang, D. Wang, D. Wang, *et al.*, "Motor network reorganization in stroke patients with dyskinesias during a shoulder-touching task: A fNIRS study," Journal of Innovative Optical Health Sciences (2023).
32. B. Sun, Z. Wu, Y. Hu, *et al.*, "Golden subject is everyone: A subject transfer neural network for motor imagery-based brain computer interfaces," Neural Netw **151**, 111–120 (2022).
33. S. V. Astafiev, C. M. Stanley, G. L. Shulman, *et al.*, "Extrastriate body area in human occipital cortex responds to the performance of motor actions," Nat. Neurosci. **7**(5), 542–548 (2004).
34. R. Oostenveld and P. Praamstra, "The five percent electrode system for high-resolution EEG and ERP measurements," Clin. Neurophysiol. **112**(4), 713–719 (2001).
35. T. Li, H. U. I. Gong, and Q. Luo, "Mcvm: Monte Carlo Modeling of Photon Migration in Voxelized Media," J. Innovative Opt. Health Sci. **03**(02), 91–102 (2010).

36. G. Derosiere, S. Dalhoumi, S. Perrey, *et al.*, "Towards a near infrared spectroscopy-based estimation of operator attentional state," PLoS One **9**(3), e92045 (2014).
37. F. A. Fishburn, R. S. Ludlum, C. J. Vaidya, *et al.*, "Temporal Derivative Distribution Repair (TDDR): A motion correction method for fNIRS," NeuroImage **184**, 171–179 (2019).
38. K. Zhao, Y. Ji, Y. Li, *et al.*, "Online Removal of Baseline Shift with a Polynomial Function for Hemodynamic Monitoring Using Near-Infrared Spectroscopy," Sensors **18**(1), 312 (2018).
39. G. Bauernfeind, S. C. Wriessnegger, I. Daly, *et al.*, "Separating heart and brain: on the reduction of physiological noise from multichannel functional near-infrared spectroscopy (fNIRS) signals," J. Neural Eng. **11**(5), 056010 (2014).
40. P. Raggam, G. Bauernfeind, and S. C. Wriessnegger, "NICA: A Novel Toolbox for Near-Infrared Spectroscopy Calculations and Analyses," Front. Neuroinform. **14**, 26 (2020).
41. S. Sasai, F. Homae, H. Watanabe, *et al.*, "A NIRS-fMRI study of resting state network," Neuroimage **63**(1), 179–193 (2012).
42. Q. Tan, M. Zhang, Y. Wang, *et al.*, "Frequency-specific functional connectivity revealed by wavelet-based coherence analysis in elderly subjects with cerebral infarction using NIRS method," Med Phys **42**(9), 5391–5403 (2015).
43. F. Al-Shargie, R. Katmah, U. Tariq, *et al.*, "Stress management using fNIRS and binaural beats stimulation," Biomed. Opt. Express **13**(6), 3552–3575 (2022).
44. M. Rubinov and O. Sporns, "Complex network measures of brain connectivity: uses and interpretations," Neuroimage **52**(3), 1059–1069 (2010).
45. L. Douw, E. van Dellen, J. C. Baayen, *et al.*, "The lesioned brain: still a small-world?" Front. Hum. Neurosci. **4**, 174 (2010).
46. D. Meunier, R. Lambiotte, and E. T. Bullmore, "Modular and hierarchically modular organization of brain networks," Front. Neurosci. **4**, 200 (2010).
47. F. A. Fishburn, M. E. Norr, A. V. Medvedev, *et al.*, "Sensitivity of fNIRS to cognitive state and load," Front. Hum. Neurosci. **8**, 76 (2014).
48. U. Braun, A. Schafer, H. Walter, *et al.*, "Dynamic reconfiguration of frontal brain networks during executive cognition in humans," Proc. Natl. Acad. Sci. U.S.A. **112**(37), 11678–11683 (2015).
49. X. Liang, Q. Zou, Y. He, *et al.*, "Topologically Reorganized Connectivity Architecture of Default-Mode, Executive-Control, and Salience Networks across Working Memory Task Loads," Cereb. Cortex **26**(4), 1501–1511 (2016).
50. C. Gao, X. Zhao, and T. Li, "Effects of indoor VOCs from paint on human brain activities during working memory tasks: An electroencephalogram study," Indoor Air **32**, e13062 (2022).
51. Y. Gao, D. Shuai, X. Bu, *et al.*, "Impairments of large-scale functional networks in attention-deficit/hyperactivity disorder: a meta-analysis of resting-state functional connectivity," Psychol. Med. **49**(15), 2475–2485 (2019).
52. H. Gu, K. P. Schulz, J. Fan, *et al.*, "Temporal Dynamics of Functional Brain States Underlie Cognitive Performance," Cereb Cortex **31**(4), 2125–2138 (2021).
53. E. Bullmore and O. Sporns, "The economy of brain network organization," Nat. Rev. Neurosci. **13**(5), 336–349 (2012).
54. G. Gong, Y. He, and A. C. Evans, "Brain connectivity: gender makes a difference," Neuroscientist **17**(5), 575–591 (2011).
55. D. Gong, H. He, W. Ma, *et al.*, "Functional Integration between Salience and Central Executive Networks: A Role for Action Video Game Experience," Neural Plast **2016**, 1–9 (2016).
56. H. Santosa, X. Zhai, F. Fishburn, *et al.*, "Quantitative comparison of correction techniques for removing systemic physiological signal in functional near-infrared spectroscopy studies," Neurophotonics **7**(03), 035009 (2020).
57. A. von Luhmann, X. Li, K. R. Muller, *et al.*, "Improved physiological noise regression in fNIRS: A multimodal extension of the General Linear Model using temporally embedded Canonical Correlation Analysis," NeuroImage **208**, 116472 (2020).